STATUS OF SARAF SUPERCONDUCTING ACCELERATION MODULE

A. Perry, Y. Ben Aliz, B. Kaizer, A. Kreisel, J. Rodnizki, L. Weissman Soreq NRC, Yavne 81800, Israel

Abstract

Soreq Applied Research Accelerator Facility (SARAF) is based on a 176 MHz superconducting RF light ions linac, currently under commissioning at Soreq NRC [1]. At present, the accelerator includes a Prototype Superconducting Module, containing 6 half wave resonators. In this work we present measurement results of various mechanical properties of the resonators. Beam operation results are also discussed, including a new technique for the calibration of the cavity pickup probe by operating the Linac using two RF sources. Lastly, simulation results obtained using CST MWS for present and future cavities are presented as well.

LORENTZ COEFFICIENT MEASUREMENTS

The electromagnetic field contained in a superconducting cavity exerts a force on the surface charges and currents developed in the conductor. This force - the radiation pressure - slightly deforms the cavity shape, thus producing a shift of the resonance frequency. That frequency shift is proportional to the square of the field and is always negative, so the resonance frequency is reduced. The proportionality constant is defined as the Lorentz coefficient K_L, so $\Delta f_c = -K_L E_a^2$, where E_a is the accelerating field and Δf_c the resonance frequency shift.

Dynamically, the radiation pressure may couple to a mechanical resonance of the cavity structure. This situation is described by the following second order differential equation:

$$\frac{d^2(\Delta f_c(t))}{dt^2} + \frac{\Omega_m}{Q_m}\frac{d(\Delta f_c(t))}{dt} + \Omega_m^2 \Delta f_c(t) = -K_L \Omega_m^2 E_a^2$$

With Ω_m, Q_m being the mode's frequency and quality factor respectively. The left hand side describes the mode of vibration and the right hand side is the Lorentz force driving term [2,3].

By linearization of the above equation around steady state values, $E_a = E_{a,0}(1 + \delta E_a)$, and application of a Laplace transformation the Lorentz Transfer Function is obtained:

$$\delta f_c(s) = \frac{-2K_L \Omega_m^2 E_{a,0}^2}{(\Omega^2 + s^2) + \frac{\Omega_m}{Q_m}s} \delta E_a \qquad (1)$$

Where $s = jw$ is the Laplace variable. This equation has a complex pole and we therefore expect a peak in the magnitude plot, accompanied by a π phase shift when crossing the resonance in frequency.

Measurement Using NWA

The Network Analyzer (NWA) is a 2-port device capable of measuring the scattering parameters (transmission, reflection) in each of its ports.

In this setup, one port of the NWA was used to drive the high power amplifier connected to one of the cavities (via a directional coupler and a circulator). The second port was connected to the cavity pick up antenna which couples to the electromagnetic field in the resonator. By generating frequency sweeps using the NWA the cavity resonance curve (transmission between the driving and pickup signals) was measured. This was done at different levels of power incident to the cavity. As can be seen in Figure [1] the high power resonance curves are 'tilted' towards the left as a result of the resonance frequency being reduced by the Lorentz force.
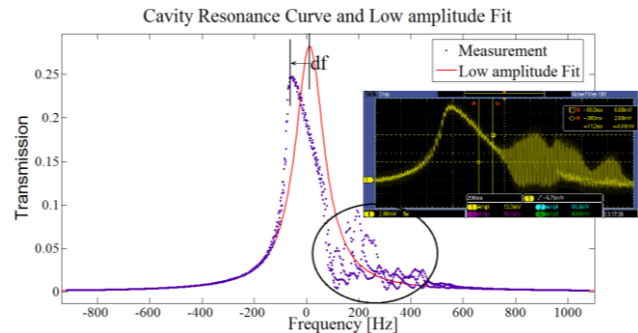
Figure 1: The cavity resonance curve measured at ~150W incident power (dots) and a fit to the low amplitudes part of the curve (Red). Marked by a circle - ripples caused by 200 Hz pondermotive oscillations observed in the scope screenshot as well.

For each resonance curve a fit was made to the low amplitudes part of the curve, to determine the resonance frequency of the cavity without the effects of the Lorentz force. Then the shift of the actual resonance frequency from that value was calculated. The amplitude of the field in the cavity was also calculated based on the pickup signal amplitude. A plot of the frequency shift Vs. the square of the accelerating field is presented in Figure [2]. This method Thus yields $K_L \sim 11.2 \pm 1.1 \frac{Hz}{\left(MV/m\right)^2}$.
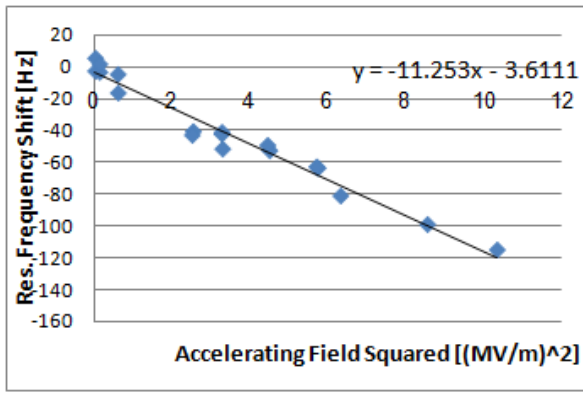
Figure 2: Frequency shift Vs. E_a^2 as measured using NWA.

As can be seen in Figure [1], above a certain power level 200 Hz pondermotive oscillations of the pickup amplitude begin to appear on the high frequency side of the resonance curve. This is an example of the Dynamic Lorentz force detuning which will be discussed in more details in a following section.

Measurement Using a PLL

In the setup described in Figure [3] the cavity is driven by a Phase Locked Loop (PLL). The PLL is a feedback system which controls the frequency of the Voltage Controlled Oscillator (VCO) in order to track the cavity resonance frequency. Changes in the VCO control voltage therefore reflect changes in the resonance frequency of the cavity.
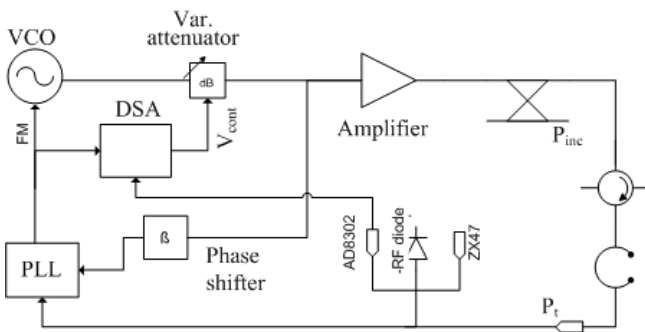
Figure 3: RF setup for the PLL measurement.

In this setup the incident power to the cavity is determined by a voltage controlled variable attenuator. The amplitude of the pickup signal from the cavity, which is proportional to the square of the field, is measured using 3 devices:
   a.   RF diode
   b.   Analog Devices AD8302 gain detector
   c.   Mini circuits ZX47 power detector.
The output signal of each device was displayed on a scope, as was also the VCO control voltage. When the power level was changed so did the amplitude of the field in the cavity and its resonance frequency – as a result of the Lorentz force; This can be observed in Figure [4].
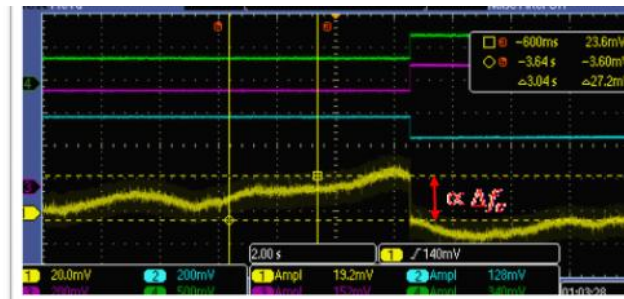
Figure 4: Change of cavity field amplitude, measured by the AD8302 gain detector (purple) ZX47 power detector (blue) and RF diode (green) resulting in a change of the resonance frequency - (VCO control voltage, Yellow).

The field amplitudes before and after the step were extracted from the pickup measurements. The resonance frequency shift due to the change of field level was obtained from the VCO control voltage. The proportionality constant between Δf_c and $\Delta\left(E_a^2\right)$ yields

$$K_L \sim 12.9 \pm 2.1\, \frac{Hz}{\left(MV/m\right)^2} \quad .$$

Dynamic Lorentz Force

The same setup as in Figure [3] was used to measure the Lorentz transfer function. Here the variable attenuator control voltage was modulated to produce a sinusoidal modulation of the incident power to the cavity and of the cavity field amplitude according to -

$$E_a(t) \propto \sqrt{P_{inc}(t)} = \sqrt{P_0(1+\varepsilon\sin(w_{mod}t))}$$

$$\sim E_{a,0} + E_{mod}\sin(w_{mod}t)$$

Under the assumption that $\varepsilon \ll 1$.

The modulating control voltage was generated by Agilent's 35670A FFT Dynamic Signal Analyzer (DSA). The output of the AD8302 gain detector and the VCO control voltage were connected to two ports of the DSA. The magnitude and phase of the transfer function between the two ports was measured using swept sine analysis for frequencies between 20 Hz and 220Hz (Figure [5]).
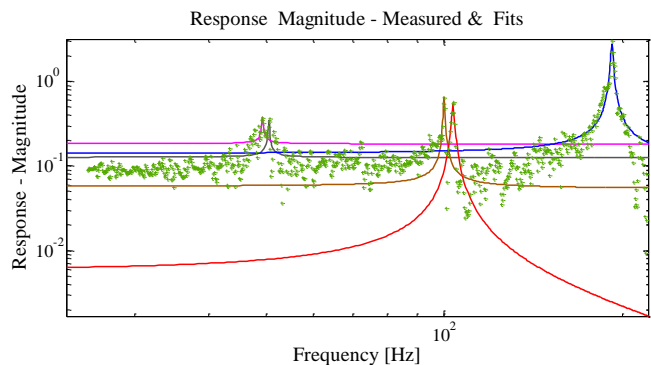
Figure 5: Measured response curve (green markers) and fits to five identified peaks near 50,100 and 200 Hz.

The response plot clearly shows peaks at frequencies near 50, 100 and 200 Hz. We interpret these peaks as mechanical resonances, although the 50 Hz peaks may also be attributed to electrical noise. The modes near 50 and 100 Hz have a double peak structure, probably related to the cylindrical symmetry of the cavity. The measured data points near each resonance were fitted to the form given by Eq. 1, and the mode's parameters were extracted (Table [1]). The value for the static Lorentz coefficient

$$K_L = \sum_i k_i \sim 5.1 \frac{Hz}{(MV/m)^2}$$ is not consistent with the

values obtained previously. This may be because of additional resonances which were not excited in the sweep. It is worth mentioning that the frequencies of these mechanical modes are especially problematic as they are located near the mains frequency (50 Hz) and its harmonics.

Table 1: Mechanical modes' parameters

	Mode 1	Mode 2	Mode 3	Mode 4	Mode 5
Ω_m [Hz]	49.3 ±0.1	50.5 ±0.1	100 ±0.1	103 ±0.2	192 ±0.1
$\frac{k_i}{Hz}$ $\overline{(MV/m)^2}$	0.42 ±0.12	0.27 ±0.14	0.38 ±0.1	0.49 ±0.2	3.5 ±0.4
Q_m	82 ±37	118 ±79	192 ±39	123 ±44	104 ±14

BEAM OPERATION

SARAF was the first accelerator to use Half Wave Resonators for the acceleration of ions [4]. Since then beam commissioning has progressed and at present the first set of target irradiation experiments is underway. Producing a high quality output beam requires setting the cavities' field levels to the values dictated by beam dynamics simulations. We now discuss a procedure for measuring the actual cavity voltage using the particle beam.

A particle with electric charge q and velocity β traversing a RF cavity receives an energy gain $\Delta E = qV_0 T(\beta)\cos\phi$ – where T is the Transit Time Factor, ϕ the phase between the beam bunches and the RF field in the cavity and V_0 the cavity voltage. Usually the cavity voltage is determined by the control system based on measurements of the RF power transmitted from the cavity via the pickup probe - P_t. That power is proportional to the square of the cavity voltage -

$V_0' \propto \sqrt{P_t} = k_t V_0$ with V_0' denoting the cavity voltage measured by the control system.

Determining the proportionality constant k_t is best done using beam based calibration. One method is by following a procedure called phasing – the phase ϕ is changed by changing the phase of the RF field in the cavity, at a set value V_0'. For each phase the energy of the particles

exiting the cavity is measured and the cosine dependence is reproduced. It is then possible to determine the value of $V_0 T$, and knowing T from beam dynamics simulations and V_0' from measurements k_t can be easily extracted.

A new technique was suggested to us by Prof. Jean Delayen. His approach was to operate the Radio Frequency Quadropole and the cavities using two different RF sources. The frequency of the particle bunches (equal to the RFQ frequency) is therefore close but not equal to the frequency of the RF field in the cavity. The outcome is that each bunch arrives to the cavity with a different random phase relative to the RF field, with the phase uniformly distributed between 0 and 2π. We can calculate the energy spectrum at the cavity output assuming that:

a. The energy distribution at the cavity input $f^i(E_i)$ is narrow enough so the Transit Time Factor can be considered the same for all particles.

b. There is no correlation between the initial energy of the particle E_i and the phase ϕ.

Under these assumptions, the probability $f^f(E_f)$ of getting a particle with a final energy E_f is equal to the probability of having E_i and an energy gain $\Delta E = Y$, such that $E_i + Y = E_f$, or:

$$f^f(E_f) = \iint f^i(E_i)f^{\Delta E}(Y)\delta(E_f - E_i - Y)dE_i dY =$$
$$= \int f^i(E_i)f^{\Delta E}(E_f - E_i)dE_i = f^i * f^{\Delta E}$$

For a uniformly distributed ϕ - $f^{\Delta E}(Y) = \frac{1}{\sqrt{(qV_0 T)^2 - Y^2}}$;

we therefore expect the energy spectrum at the cavity output to have two distinct peaks separated by a distance $2qV_0 T$ (because $f^i(E_i)$ is approximately a Gaussian distribution). Measuring that distance and knowing the theoretical value of T the actual cavity voltage V_0 can be deduced and the probe reading scaled accordingly.

The output energy spectrum was measured using Rutherford scattering off a gold foil [5]. The scattered particles' energy had been measured using a Silicon detector. A typical spectrum is shown in Figure [6].
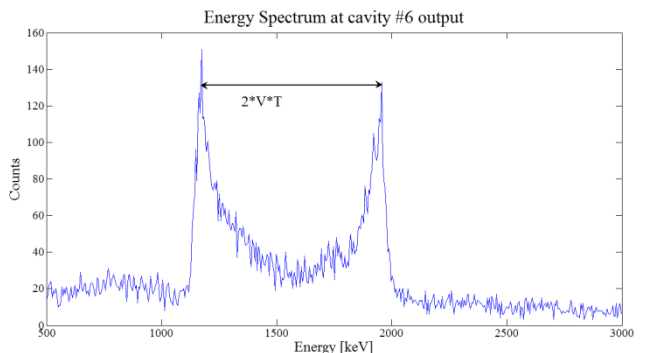
Figure 6: Measured energy spectrum at cavity #6 output.

For each cavity the set voltage V_0' was changed in the control system and a spectrum was measured for each value. The value of $2V_0T$ was then extracted from the different spectra and a plot of V_0T Vs. V_0' was generated for that cavity. Knowing V_0T/V_0' and $T(\beta)$ the calibration k_t is possible. The uneven distribution around the initial energy of 1.5 MeV stems from the velocity dependence of the Transit Time Factor. By accounting for this effect a better calibration can be achieved.

CST MWS SIMULATIONS

The Superconducting part of SARAF Phase I is composed of a single cryostat, the Prototype SC Module (PSM) containing six SC Half Wave Resonators and three SC solenoids. The PSM was designed to accelerate 2mA Proton and Deuteron beams from 1.5 MeV/u to 4-5 MeV respectively.

An extension of the Linac up to an energy of 40 MeV is planned (Phase II), while a redesign of the Radio Frequency Quadropole is considered as well. This redesign may result in the RFQ output energy being slightly reduced to less than the present 1.5 MeV/u.

The above modifications will exact the introduction of new accelerating structures. It is conceived that two types of cavities will be used: one with a geometrical beta of 0.085 and the second with $\beta = 0.13$.

A preliminary design of a $\beta = 0.13$ Half Wave Resonator is described in the following section. Electromagnetic simulations using CST MicroWave Studio were performed, from which the cavities' figures of merit were extracted. These simulation results will be used for constructing a lattice for the Linac extension to 40 MeV.

CST MWS Eigenmode solver and Mechanical solver were also used in order to generate an Electro-Mechanical simulation of SARAF's existing half wave resonators. The sensitivity to He pressure fluctuations was extracted and compared to the measured value, as shown in a separate sub-section.

Design and Simulations of $\beta = 0.13$ Cavity

Several other facilities, including IFMIF [6] and Eurisol [7], have presented in the past designs for Half Wave Resonators with similar frequencies and beta values. Our design relies on Eurisol's $\beta = 0.13$ cavity. However, as suggested by Zaplatin [6], we use a conical inner conductor, round beam ports and round domes (Figure [7]). The diameters of the conical inner conductor was optimized to reduce the values of the peak fields, at the expanse of reducing the normalized shunt impedance as well. Figures of merit for this preliminary design are reported in Table [2]. Design work will continue in the future, including further optimization, mechanical analysis, addition of a coupler, tuner and Helium Vessel and fabrication, assembly and cleaning considerations.

Electro-Mechanical Simulations of SARAF's $\beta=0.09$ Cavities

The existing $\beta=0.09$ HWRs have a very high sensitivity to external pressure variations, measured at $\frac{df}{dP} \sim 60 \frac{Hz}{mBar}$. CST MWS was used to generate an Electro-Mechanical simulation of the cavity in order to numerically evaluate that coefficient. The cavity model was input to CST's Mechanical solver and a uniform pressure vector was applied to its surface. The displacements of the surface elements as a result of the force acting on them had been calculated by the solver (Figure [8]). The deformed structure was then input to CST's EM solver and its resonance frequency was calculated and compared to that of the original non-deformed model. The simulated value $\frac{df}{dP} \sim 30 \frac{Hz}{mBar}$ is only half of the experimentally measured one. However, it is also very dependent on the mechanical boundary conditions used in the simulation, which may account for the difference.
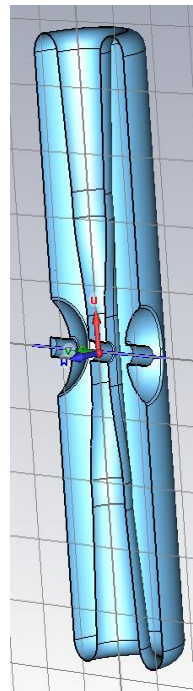
Parameter	Value	Units
β	0.13	
R/Q_0	231	Ω
G	43	Ω
E_p/E_a	4.13	
B_p/E_a	9.3	$\frac{mT}{MV/m}$
ω_0	176	MHz
$L_{acc} = \beta\lambda$	221	mm
L_{re}	260	Mm

Figure 7: Table 2: $\beta =0.13$ CST MWS model (Left) and simulated figures of merit (Right).
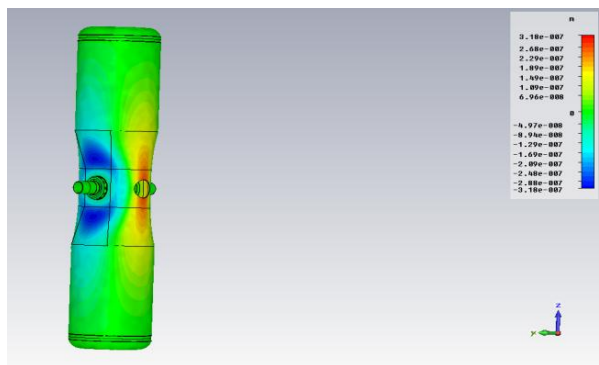
Figure 8: Surface elements displacements calculated by CST Mechanical solver.

SUMMARY AND OUTLOOK

The performance of SARAF's superconducting Half Wave Resonators is mainly limited by their inherit mechanical stability problems. This is manifested in the high static Lorentz coefficient, high sensitivity to external pressure fluctuations and the ill-placed mechanical resonances. Nevertheless, beam operation is possible with the cavities working at gradients below their design values.

While improving the stiffness of the cavity structure is a possibility which may be explored in the future, SARAF's SRF team faces several other upcoming activities which will hopefully contribute to performance. These includes the upgrade of the RF system, including the integration of new 4kW high power amplifiers; Testing of a new algorithm for the control of the piezoelectric tuner, implemented on a FPGA core, is also planned.

In parallel to that, additional simulation tools and capabilities are being acquired. A complete mechanical analysis of the cavity structure using ANSYS will be performed and compared to available experimental data. Work on the design, both Electromagnetic and Mechanical, of new HWRs for Phase II will continue as well.

Finally, plans for the construction of a SRF test facility dedicated to maintenance and testing of superconducting cavities are already being discussed.

REFERENCES

[1] L. Weissman "THE STATUS OF THE SARAF LINAC PROJECT", Linac10, Tsukuba, Japan, September 2010, WE102.

[2] J. R. Delayen "Ponderomotive instabilities and microphonics — a tutorial", Physica C 4411-6 (2006).

[3] A. Neumann, "Compensating Microphonics in SRF Cavities to ensure beam stability for future Free-Electron-Lasers", thesis dissertation, Humboldt University of Berlin, April 2008.

[4] I. Mardor, "the SARAF CW 40 MeV Proton/Deuteron Accelerator", SRF'09, Berlin, July 2009, THZCH03.

[5] L. Weissman, " First Experience at SARAF with Proton Beams using the Rutherford Scattering Monitor", DIPAC'09, Basel, May 2009, TUPB20 (2009).

[6] E. Zaplatin, " IFMIF-EVEDA SC $\beta = 0.094$ HALF-WAVE RESONATOR STUDY", SRF'09, BERLIN, JULY 2009, THPPO015.

[7] A. Facco, " DESIGN OPTIMIZATION OF THE EURISOL DRIVER LOW-BETA CAVITIES".